Contents lists available at ScienceDirect

Chemosphere

journal homepage: www.elsevier.com/locate/chemosphere

Assessing nitrate groundwater hotspots in Europe reveals an inadequate designation of Nitrate Vulnerable Zones

J. Serra [a,*], C. Marques-dos-Santos [a], J. Marinheiro [a], S. Cruz [a], M.R. Cameira [b], W. de Vries [c], T. Dalgaard [d], N.J. Hutchings [d], M. Graversgaard [d], F. Giannini-Kurina [d], L. Lassaletta [e], A. Sanz-Cobeña [e], M. Quemada [e], E. Aguilera [e], S. Medinets [f,g], R. Einarsson [h], J. Garnier [i]

[a] Forest Research Centre CEF, Associate Laboratory TERRA, Instituto Superior de Agronomía, Universidade de Lisboa, 1349-017, Lisbon, Portugal
[b] LEAF-Linking Landscape, Environment, Agriculture and Food-Research Center, Associated Laboratory TERRA, Instituto Superior de Agronomia, Universidade de Lisboa, Tapada da Ajuda, 1349-017, Lisbon, Portugal
[c] Environmental Systems Analysis Group, Wageningen University and Research, Wageningen, the Netherlands
[d] Department of Agroecology, Aarhus University, Blichers Allé 20, DK-8830, Tjele, Denmark
[e] CEIGRAM/ETSIAAB, Universidad Politécnica de Madrid, 28040, Madrid, Spain
[f] Odesa National I. I. Mechnikov University, 7 Mayakovskogo lane, 65082, Odesa, Ukraine
[g] UK Centre for Ecology & Hydrology (Edinburgh), Bush Estate, EH26 0QB, Penicuik, UK
[h] Department of Energy and Technology, Swedish University of Agricultural Sciences, Uppsala, Sweden
[i] SU CNRS EPHE, UMR Metis, 7619, Paris, France

HIGHLIGHTS

- NO_3^- concentrations in groundwater mapped at a detailed spatial resolution.
- The effectiveness of the Nitrates Directive in reducing NO_3^- hotspots was assessed.
- Limited success of the Nitrates Directive, particularly in Southern Europe.
- Less than half of NO_3^- hotspots in groundwater covered by the designated NVZs.

GRAPHICAL ABSTRACT
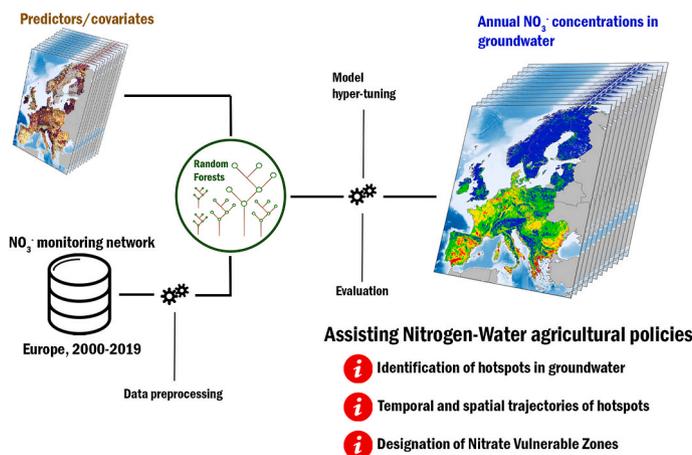
ARTICLE INFO

Handling Editor: Jun Huang

ABSTRACT

Monitoring networks show that the European Union Nitrates Directive (ND) has had mixed success in reducing nitrate concentrations in groundwater. By combining machine learning and monitored nitrate concentrations (1992–2019), we estimate the total area of nitrate hotspots in Europe to be 401,000 km², with 47% occurring

* Corresponding author.
  E-mail address: jserra@isa.ulisboa.pt (J. Serra).

outside of Nitrate Vulnerable Zones (NVZs). We also found contrasting increasing or decreasing trends, varying per country and time periods. We estimate that only 5% of the 122,000 km² of hotspots in 2019 will meet nitrate quality standards by 2040 and that these may be offset by the appearance of new hotspots. Our results reveal that the effectiveness of the ND is limited by both time-lags between the implementation of good practices and pollution reduction and an inadequate designation of NVZs. Substantial improvements in the designation and regulation of NVZs are necessary, as well as in the quality of monitoring stations in terms of spatial density and information available concerning sampling depth, if the objectives of EU legislation to protect groundwater are to be achieved.

1. Introduction

Concern over groundwater nitrate (NO_3^-) contamination from agriculture led to the establishment of the European Union Nitrates Directive (ND) in 1991, the Drinking Water Directive in 1998 and the Groundwater Directive in 2006 (Wuijts et al., 2021). In accordance with these framework policies, Member States (MS) are required to address excessive NO_3^- leaching from areas of intensive agriculture (de Vries et al., 2021) by designating areas at risk of NO_3^- pollution ($\geq$50 mg L^{-1}) as Nitrate Vulnerable Zones (NVZ). The ND requires the implementation of Action Programmes with mandatory measures to reduce NO_3^- losses in the NVZs, such as limits on nitrogen (N) fertilisation rates, which can be effective in reducing NO_3^- losses (D'Haene et al., 2014).

The ND allows MS some flexibility in how to meet the main objective of reducing NO_3^- pollution (Beusen et al., 2015), leading to variations in the criteria for designating NVZs (Arauzo, 2017). The effectiveness of NVZs in reducing NO_3^- pollution relies on an evidence-based delineation (Arauzo et al., 2022) and on implementing strategies tailored to local conditions (Quemada et al., 2013). The NVZ delineation depends not only on the criteria used but also on (environmental) political ambitions (European Commission, 2018) and the administrative difficulties associated with a partial designation of the territory. Ambitious delineations that cover the whole territory are implemented only in 10 MS as of 2023. For the remaining MS, it is possible that the NVZs do not cover all of the groundwater NO_3^- hotspots in groundwater. Despite the long-term implementation of the ND and related policies, groundwater NO_3^- pollution remains a challenge with many MS struggling to meet the ND standards (European Commission, 2021). While the ND does not establish any deadline to meet water quality objectives, good ecological and chemical status must be achieved by 2027 according to the Water Framework Directive (European Commission, 2021).

The identification of NVZs (Arauzo et al., 2017; 2022; Cameira et al., 2021) and groundwater pollution hotspots (Jain, 2023) typically rely on index-based conceptual approaches, although simulation models (e.g., Szalińska et al., 2018) and other concepts (e.g., grey water footprint; Serio et al., 2018) have also been used. There are other index-based approaches that mainly focus on the agricultural hazard, groundwater vulnerability or the risk of NO_3^- contamination. In this context, agricultural hazard can be defined as land use ratings for N loads (Kazakis and Voudouris, 2015), estimated N surplus (Cameira et al., 2019) or an estimated NO_3^- concentration in the potential aquifer recharge from below the root zone (Serra et al., 2021). Although the impact of other sources of hazard on groundwater NO_3^- contamination, such as urbanization/industrialization, which can be large e.g., in China (Zhang et al., 2020; Huang et al., 2018), is limited in Europe due to a much slower expansion of built-up areas and the strong development of sanitation infrastructure. The definition of groundwater vulnerability varies between methods (e.g., DRASTIC, susceptibility index) (Fannakh and Farsang, 2022) but aims to highlight regions where NO_3^- is more likely to reach groundwater. The risk of NO_3^- contamination is a function of the agricultural hazard and groundwater vulnerability (Serra et al., 2021) or the risk associated with soil permeability (Arauzo et al., 2022). However, these approaches are unable to directly predict groundwater NO_3^- concentrations, often only providing a qualitative assessment of the risk of contamination. The methodologies used to designate NVZs in the

different countries are also often not transparent with few published studies (e.g., England; DEFRA, 2016).

Recently, machine learning models such as random forests (RF) have been applied to predict NO_3^- concentration in groundwater (Knoll et al., 2019, 2020; Karimanzira et al., 2023; Deng et al., 2023; Haggerty et al., 2023), thus allowing to benchmark NVZs. Using this approach offers a threefold advantage: (i) direct prediction (and validation) of NO_3^- concentrations in groundwater, (ii) extending predictions to regions with less detailed, scarce or no data and (iii) enhanced large-scale monitoring of groundwater NO_3^- concentrations, which allows the detection of whether the groundwater quality target of 50 mg L^{-1} per the ND is being met in the designated NVZs.

Trend analyses of NO_3^- concentrations in groundwater are commonly based on observations from monitoring stations (Hansen et al., 2012). However, monitoring networks may fail to cover all hotspots in Europe and not all stations provide complete time series, limiting the quality of the analyses. This impacts the effectiveness of the designated NVZs in addressing the full extent of hotspots across all Europe. Coupling machine learning algorithms with monitoring networks can uncover undetected hotspots while providing complete temporal coverage. Here we hypothesize that by introducing spatiotemporal predictors into machine learning models, we can reduce the spatial and temporal constraints imposed by monitoring networks when regulating groundwater quality. This enables an enhanced assessment of the effectiveness of the ND in reducing groundwater NO_3^- hotspots.

We do this by implementing a random forest (RF) model to predict annual NO_3^- concentration in groundwater in Europe for the period 1992–2019 at high spatial resolution (0.04°x0.04°; ~3 km × 3 km). We use the RF model to (i) generate spatially explicit predictions of trends in NO_3^- concentrations in groundwater across Europe, starting from the implementation of the ND to understand how NO_3^- concentrations have responded to the national policies and regulations, (ii) assess whether the current NVZs cover all the areas threatened by NO_3^- pollution, and (iii) estimate the necessary reductions in NO_3^- concentrations to meet water quality standards. By doing so, this study aims to contribute to a potential improvement of the effectiveness of water and agrienvironmental policies.

2. Methods

2.1. Combining random forests with monitoring networks

We implemented a random forest (RF) model to predict annual NO_3^- concentration in groundwater at 0.04°x0.04° in Europe (European Union plus Norway, Switzerland and the United Kingdom) for the period 1992–2019, totalling 835,644 cells. This model was previously used to predict annual concentrations in Europe at 10 km × 10 km for 2000–2010 (Serra et al., 2023a) with a R² of 0.65 ± 0.08. We improved this framework by training the model with stations from the period 2000–2019 rather than for individual years; that is, a single model was used to predict concentrations across Europe. This allowed it to overcome the limitations imposed by a restricted spatial coverage of the monitoring stations, which cover only the most problematic areas in terms of NO_3^- pollution in early years (e.g., 1990s/early 2000s) (Serra et al., 2023a, b).

We collected data of groundwater monitoring (coordinates, sampling date/year, concentration) stations across Europe from the European Environmental Agency Waterbase (https://www.eea.europa.eu/data-and-maps/data/waterbase-water-quality-icm-2). We used the annual data for the period 2000–2019 to train the RF model, totalling 238,755 data points from 23,267 stations. We averaged the annual data for the stations containing more than one record per year.

We extracted data from 152 explanatory predictors ($0.04°x0.04°$) that may influence NO_3^- concentration in groundwater for each station (Table S1). The selection of each predictor was made according to the following criteria: (i) the predictor should play a role in NO_3^- leaching dynamics between below the root zone and the phreatic zone, (ii) the original spatial resolution must have been 10 km × 10 km or less, (iii) management related predictors that vary annually/seasonally (e.g., irrigation, fertilisation) were available for the period 1992–2019 and (iv) the predictor was publicly available. We first selected the predictors based on previous studies (e.g., Ransom et al., 2022; Ouedraogo et al., 2019; Serra et al., 2023a; Spijker et al., 2021; Wick et al., 2012) and checked whether these were in line with the remaining criteria. Table S1 shows the final predictors used in the model as well as their rationale for their selection. We included the year of simulation and latitude/longitude as predictors to better account for spatiotemporal variation. We also recognise that some potentially important predictors were excluded because they did not meet all the criteria. These included wastewater treatment and reuse (available only for the year 2015; Jones et al., 2021), N loads from wastewater (available only for the 2010s; Vigiak et al., 2020) and sector water withdrawals (e.g., spatial resolution of about 50 km × 50 km and timeperiod was only until 2010; Huang et al., 2018).

We partitioned the dataset into training (80%) and testing (20%) subsets. The model hypertuning focussed on the number of predictors in a decision tree (45, 55 or 65), the number of trees from an out-of-bag sample (500, 750, 1000, 1500, 2000 and 3000) and node size (2 and 5). The best model, based on the lowest out-of-bag mean square error, was achieved for 65 predictors, 2000 trees and 2 nodes.

2.2. Hotspot identification

We defined hotspot areas as a $0.04°x0.04°$ grid cell with a predicted concentration of above 50 mg NO_3^- L^{-1} as per the ND. Here we use the most recent spatial data of the NVZs (EEA, 2021; Fig. S1) to uncover whether these are effectively tackling the most pressing areas in terms of groundwater pollution. Although the NVZs have been expanding since 1991, both in terms of area and spatial coverage as more countries joined the EU, EEA (2021) does not specify such data nor were we able to source it from elsewhere. We defined two different periods (1992–2003 and 2004–2019) to perform trend analysis (see below) and quantify hotspot areas. The year 2003 was chosen as a break point since some countries started to implement the whole territory approach (e.g., Austria, Ireland). We acknowledge other important years (e.g., establishment of the monitoring programmes in 2007). Knowing the (i) location and area of the hotspots per country and (ii) the designated NVZs, we computed the hotspot coverage of the NVZs for a given country:

$$Hotspot_{coverage} = \frac{\sum_{i=1992}^{2019} Hotspots_{NVZ,i}}{\sum_{i=1992}^{2019} Hotspots_{Country,i}} \qquad \text{Eq. (1)}$$

where i corresponds to each year, $Hotspots_{NVZ}$ (km^2) and $Hotspots_{Country}$ (km^2) refers to the total area of hotspots in a NVZ and country for the period 1992–2019, respectively.

2.3. Estimating the time and reduction in concentrations required for compliance with groundwater quality objectives

We estimated the time required until hotspots are able to comply with the groundwater quality objective of 50 mg L^{-1}. To do so, we selected cells where (i) the NO_3^- concentration was above the 50 mg L^{-1} threshold in 2019 and (ii) with a declining trend for the period 2004–2019 per the Sen's slope:

$$T_{NR} = \left(N_{Hconc,2019} - 50 \right) / SS_{04-19} \qquad \text{Eq. (2)}$$

where T_{NR} is the time necessary for the reduction until groundwater NO_3^- concentration complies with the ND (yr), $N_{Hconc,2019}$ is the groundwater NO_3^- concentration above 50 mg L^{-1} that attained a declining Sen Slope during 2004–2019 (mg L^{-1}) and SS_{04-19} is the Sen Slope attained for the period 2004–2019 (mg L^{-1} yr^{-1}). Similarly, we quantified the appearance of new hotspots by using current concentrations (below 50 mg L^{-1}) with increasing trends by adapting Eq. (2):

$$T_{NH} = \left(50 - N_{conc,2019} \right) / SS_{04-19} \qquad \text{Eq. (3)}$$

where T_{NH} is the time of the appearance of a new hotspot (yr) and $N_{conc,2019}$ is the groundwater NO_3^- concentration below 50 mg L^{-1} that attained an increasing Sen Slope during 2004–2019 (mg L^{-1}). We complemented this with an analysis of the required annual reduction that enables hotspots in 2019 to comply with water quality objectives in target years: 2027 (target year of the Water Framework Directive) and 2040 (long-term horizon):

$$Nec_{reduction_{TY}} = \left(N_{conc,2019} - 50 \right) / (TY - 2019) \qquad \text{Eq. (4)}$$

where TY is the target year (2027 or 2040), $NEC_{reductionTY}$ is the necessary reduction in groundwater NO_3^- concentration (mg L^{-1}) and $N_{conc,2019}$ is the groundwater NO_3^- concentration that attained a declining Sen Slope during 2004–2019 (mg L^{-1}).

2.4. Uncertainty analysis

We performed an uncertainty analysis using the hyper-tuned random forest model. We focussed on the predictors more directly affected by the ND (here referred to as N predictors): the N surplus, total N inputs from manure and from fertilisers to crop- and grassland. To explore the uncertainty of NO_3^- concentrations related to the N predictors, we multiplied each predictor by 0.75, 0.9, 0.95, 1.05, 1.1 and 1.25 on a yearly basis. We calculated the number of hotspots in each uncertainty simulation at the European and national levels and compare those data with the baseline.

2.5. Scenario analysis

We implemented a scenario analysis where annual NO_3^- concentrations were predicted using the hyper-tuned model for two different scenarios: historical (post Green Revolution) and present. For the historical and present scenarios, we averaged the N predictors for 1961–1990 and 2000–2019, respectively. This aimed (i) to take advantage of our predictive approach to explore the impact that alternative management scenarios may have had on groundwater NO_3^- concentrations and hotspot area at the national scale while (ii) disentangling the possible effects of the ND on the N predictors. We recognise the implicit impact that the ND may have had on others, such as land use (rainfed and irrigated crops) and soil organic carbon.

2.6. Statistical and trend analyses

In addition to R^2 and root mean squared error (RMSE), the performance of the final model was evaluated using the modified version of the Kling-Gupta Efficiency (KGEM), which includes bias (β), correlation (r)

and variability (γ) (Dorado-Guerra et al., 2022):

$$KGEM = 1 - \sqrt{(r-1)^2 + (\beta-1)^2 + (\gamma-1)^2} \qquad \text{Eq. (5)}$$

where r is the correlation coefficient between the simulation and observations, β refers to the bias, calculated as the ratio between the simulated and observed means and γ is the ratio between the coefficient of variation of the simulation and observations.

We carried out trend analysis for the three periods (1992–2003, 2004–2019 and 1992–2019) at the grid and national/European levels. We used the non-parametric Mann-Kendall test at 95% significance level to detect significant trends and Sen's slope to estimate trend magnitude. We applied the ANOVA and Tukey test to explore statistical differences in the scenarios. We also applied Spearman's rank correlation coefficient as another non-parametric measure of rank correlation to identify monotonic functions. We detected outliers in the timeseries of hotspots at the national and grid levels using Hample filter as points outside the ranged composed by the median ±3 median absolute deviations (Pearson et al., 2016).

3. Results & discussion

3.1. Model performance

The RF model attained a predictive performance of a R^2 of 0.81, a RMSPE of 12.7 mg NO_3^- L^{-1} (hereafter units are only expressed as mg L^{-1}), β of 1.0, γ of 0.85 and a modified Kling-Gupta Efficiency (KGEM) of 0.77. The overall performance showed two distinct periods over time: it first increased until 2010 but then it declined (Fig. 1a). The model underperformed between 2011 and 2015 as it was unable to predict high concentrations (>200 mg L^{-1}) in Greece and Italy (Figs. S2–3) as evidenced by the increase in RMSPE to 30 mg L^{-1} in 2014 and the sharp decline of KGEM. The most important predictors in the RF model are showed in Fig. S4, although it is worth noting that no N predictor was in the top ten predictors.

The marked differences in the performance over time are explained by annual differences in the number of data points in the testing partition, as well as their spatial coverage. For instance, the average number of data points for the period 2000–2010 (n = 3364) is more than double of the period 2000–2019 (n = 1541) (Figs. S5–7). The testing partition for the former period also has a wider spatial coverage, while the latter mostly focusses on a few countries (Fig. S8). This implies that the predictions may contain biases introduced by differences in the annual data points in the model training and subsequent validation in the testing partition. Indeed, the number of annual data points in the testing partition and the prediction year explained a large portion of the variance of the performance metrics, from 64% concerning the RMSE to 79% concerning the KGEM (Table S2). The implications of these biases in the predictions are further discussed in section 3.6 of this paper.
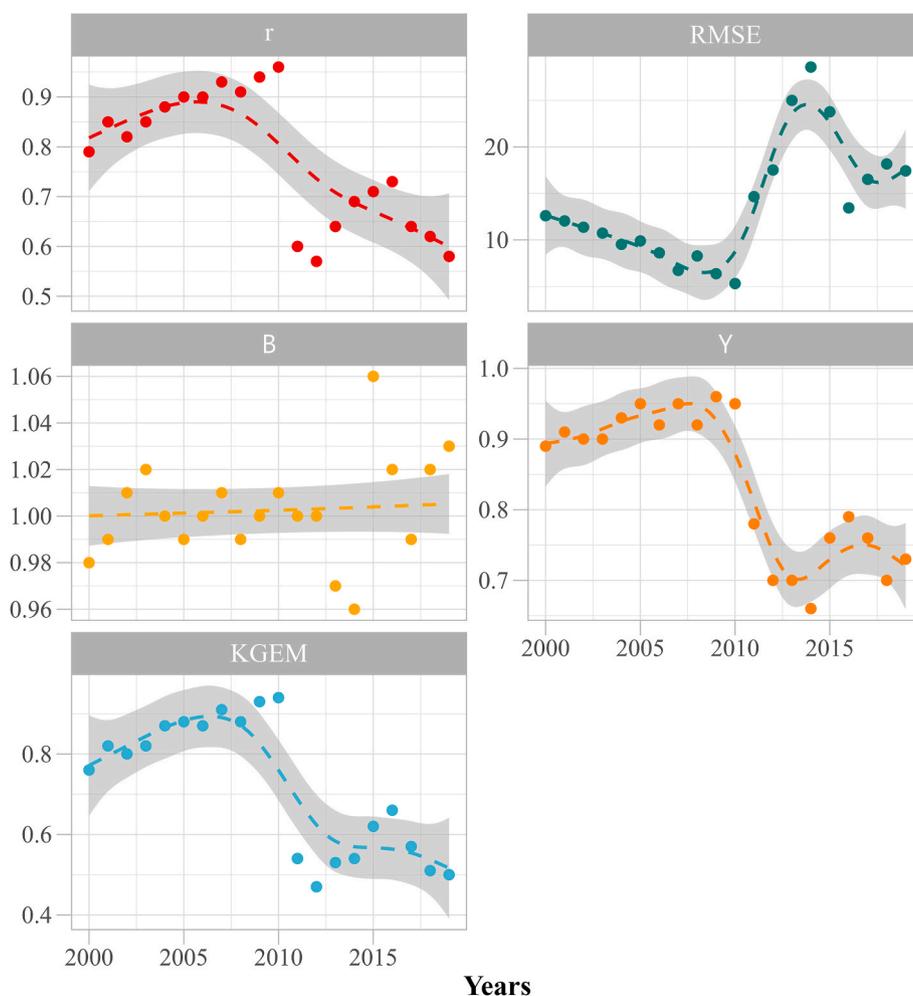

Fig. 1. (a) Annual performance metrics (2000–2019) in the testing partition of the random forest model, namely correlation (r), RMSPE, bias (*β*), variability (*γ*), modified Kling-Gupta Efficiency (KGEM). The dotted lines represent a generalized additive model for the different performance metrics.

3.2. Spatial and temporal patterns of groundwater nitrate concentrations in Europe

Fig. 2 shows the surface area of annual hotspots in Europe, which was about 107,000 ± 42,000 km² yr⁻¹ (mean ± SD for the period 1992–2019 hereafter). The area of hotspots in Europe increased at a rate of 1219 km² yr⁻¹ (CI95%: 212–2226; $p = 0.44$). The period 1992–2003 showed a declining trend with a contraction in hotspot area of 2250 km² yr¹ (CI95%: 5704–1666; $p = 0.024$). We found a contrasting trend for the subsequent period pf 2004–2019 where hotspot area in Europe increased 7200 km² yr¹ (CI: 5010–9324; $p = 0.001$).

We detected a number of years where the hotspot area in Europe are likely overestimated (Fig. 2 and Figs. S9–10), particularly in 1994 (175,000 km²), 2015 (259,000 km²) and 2018 (142,000 km²). This is because the model overestimated groundwater NO_3^- concentrations in specific regions/countries in some years such as Mediterranean Europe (Spain, Italy and Croatia) in 2015 and Eastern Europe (Romania and Bulgaria) in 1994 (see below).

Our simulation identified hotspots scattered across Europe (Fig. 3), with four distinct regions standing out: (i) Southern/Mediterranean Europe with an emphasis on Spain (e.g., Ebro and Guadalquivir basins) and in the coastal regions in Southern Italy and Greece; (ii) Northwestern Europe, covering the European plains from Normandy (NW France) to Denmark; (iii) Central Europe around Austria, Czech Republic and Slovakia and (iv) Eastern Europe with a hotspot covering a large area of Bulgaria and Romania.

We compared our predictions with the ND Report for the period 2016–2019 (European Commission, 2021; Figs. S11–12), which revealed some discrepancies in the number of stations, spatial coverage and NO_3^- concentrations. The dataset from EEA Waterbase has large gaps in Normandy (Garnier et al., 2023), an important agriculture hotspot in France, Hungary, Croatia and Greece, resulting in artificial predictions for these regions due to the lack of ground-truths to train/test

the model. We were able to ascertain that the model is likely overestimated in Southern Croatia and showed mixed results in Northeastern Europe, correctly identifying two hotspots (Ondrasek et al., 2021; Brkić et al., 2021) but also overestimated groundwater NO3- concentrations by about 10–15 mg L-1 near the border with Hungary (Brkić et al., 2019). Concentrations may have been underestimated in the UK, as European Commission (2021) reported several monitoring stations with concentrations above 50 mg L⁻¹, while less than 1% of the training data here (n = 18,000) exceeded this threshold. This emphasizes that the data available from the monitoring stations is itself a major source of uncertainty in the predictions and their ability to reflect reality. In addition, it is difficult to ensure quality control due to measurement errors/instrumentation issues and sampling biases. Our findings underscore the need for an open access to all sampling points in the EEA Waterbase dataset, despite confidentiality restrictions, to improve the accuracy and reliability of future predictions (see Section 4 of the Supplementary Text).

Our trend analysis revealed contrasting trajectories of NO_3^- concentrations in groundwater across different regions over three time periods (Fig. 4). We found that statistically significant trends, either increasing or decreasing, covered an area of 1877,000 km² (52% of total land area) across Europe during 1992–2019. The decreasing trends accounted for 1698,000 km² (47%), with reductions below 0.5 mg L⁻¹ yr⁻¹ in about 1600,000 km². Conversely, we identified increasing trends in 179,000 km², 68% of which showed an increase below 0.3 mg L⁻¹ yr⁻¹. However, a substantial shift occurred between 1992-2003 and 2004–2019. The area with decreasing trends was reduced from 932,000 to 340,000 km², while the area with increasing trends expanded 30-fold, from 28,000 to 839,000 km², respectively for the two periods.

We examined the spatial variation in the trends (Fig. 4) and identified an aggravation of NO_3^- contamination in the coastal regions around the Mediterranean Sea (Spain, France, Italy and Greece) and Eastern Europe. In Greece, we found a considerable expansion of areas with high
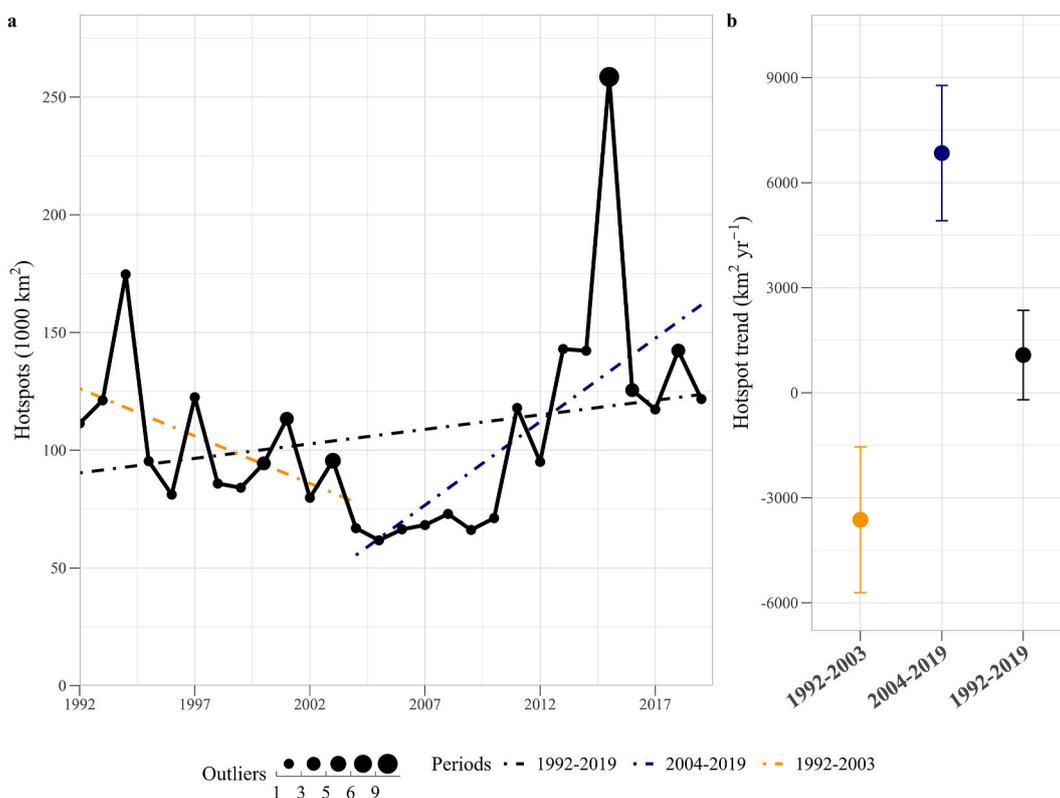

Fig. 2. The area of annual hotspots for three periods (1992–2019, 1992–2003 and 2004–2019) and respective Sen's slopes (±95% CI) are displayed in a) and b), respectively. The different lines in a) represent the linear regression with (continuous) and without (dashed) the year 2015. Outliers represent the number of countries were outliers were detected in the timeseries of hotspot area.
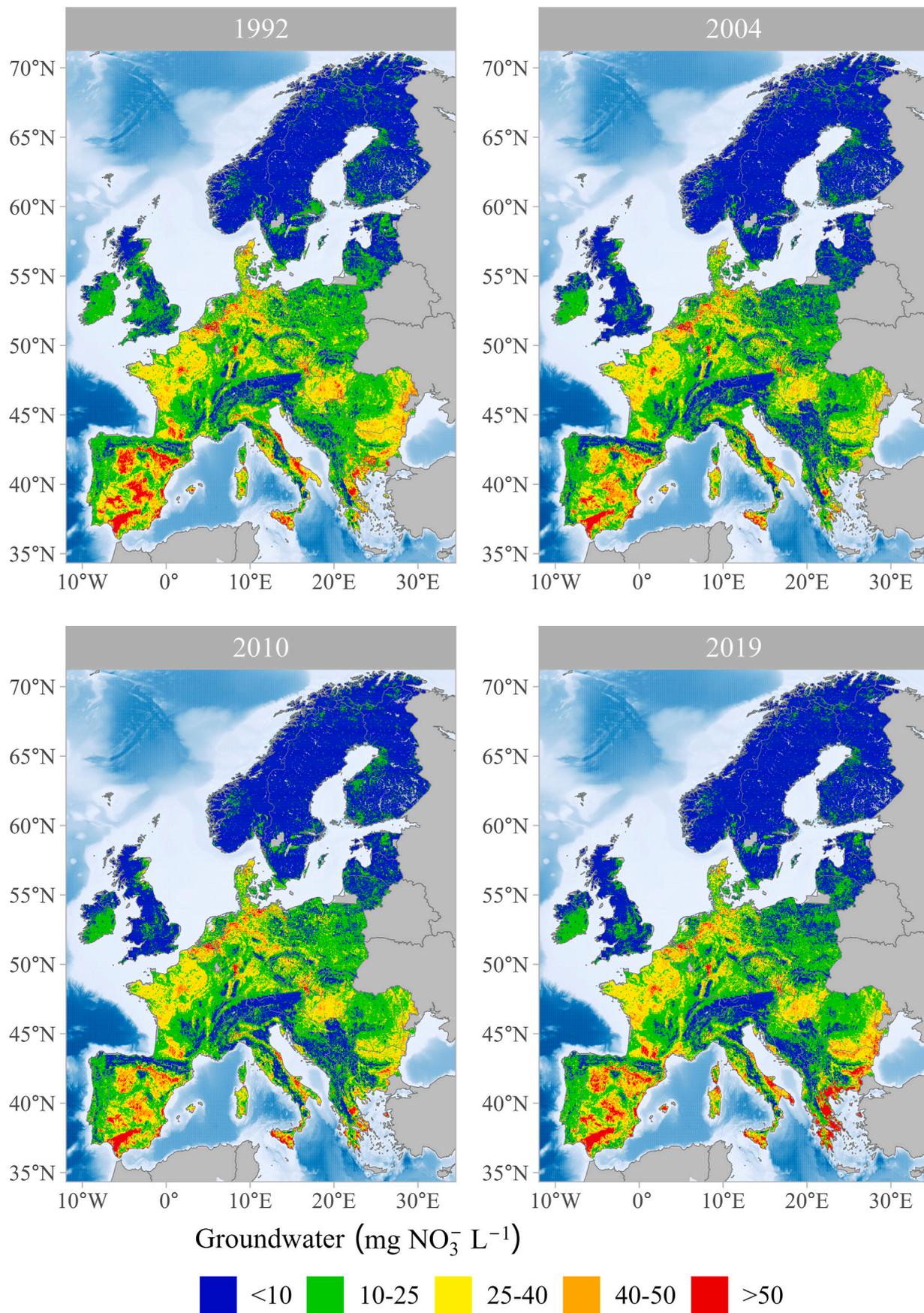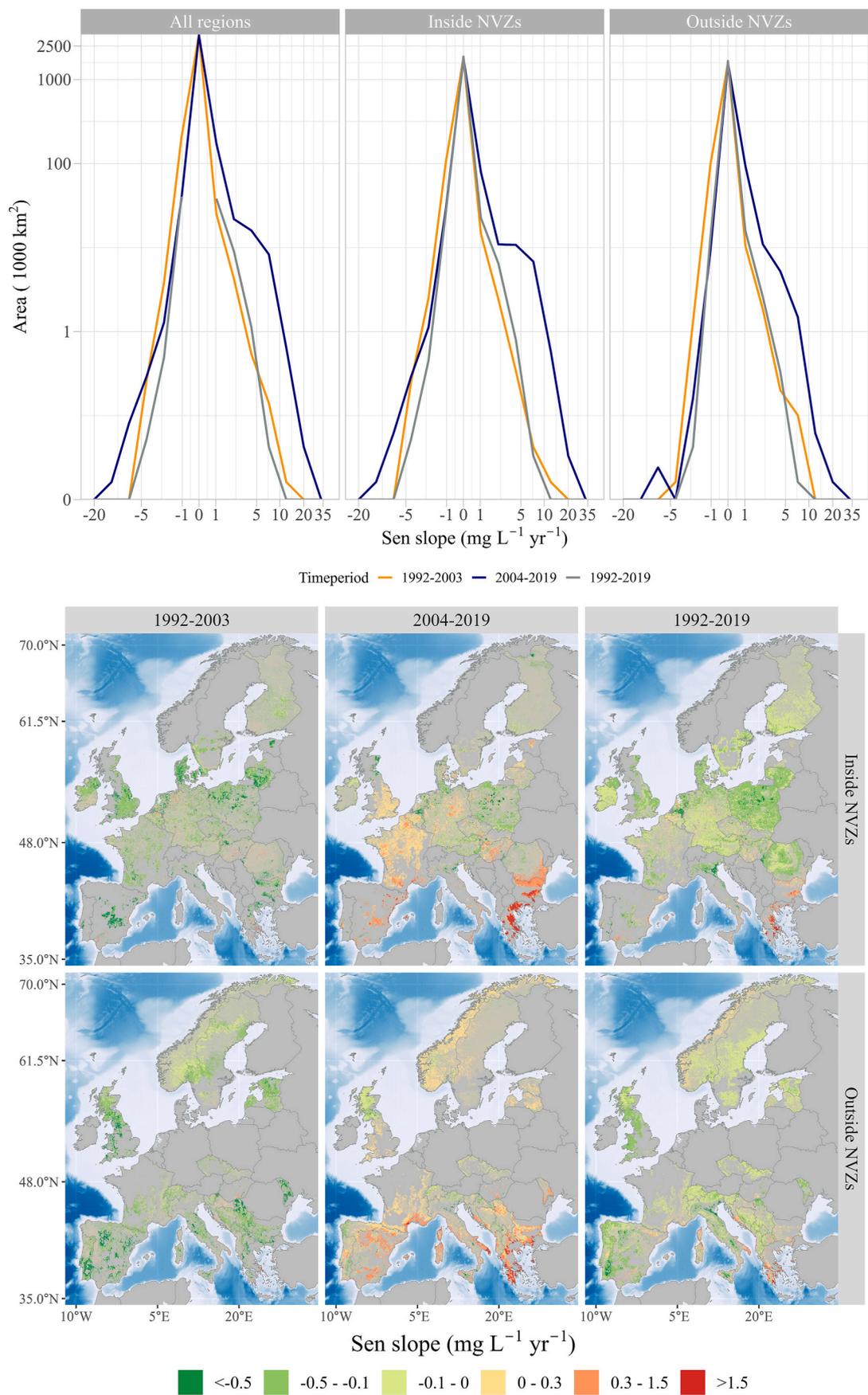
Fig. 3. Groundwater nitrate concentration predicted for snapshot years in Europe at 0.04°x0.04°. Hotspots, defined as concentrations above 50 mg L^{-1}, according to the Nitrates Directive, are highlighted in red. (For interpretation of the references to colour in this figure legend, the reader is referred to the Web version of this article.)

Fig. 4. a) Variability distribution of trends in nitrate concentration in groundwater, per the Sen slope, inside and outside NVZs across three different periods: 1992–2003, 2004–2019 and 1992–2019 using a pseudo logarithmic scale. The spatial distributions (also including all cells) are displayed in b). Non-statistically significant trends are displayed with more transparency.

rates of increase (>1.5 mg L^{-1} yr^{-1}) of 30,000 km^2 (4000 to 34,000) between 1992-2003 and 2004–2019, the largest in Europe. We also identified a large shift in the trend in Spain where 93,000 km^2 attained a moderately high increase in NO$_3^-$ concentrations (0.3–1.5 mg L^{-1} yr^{-1}) during 2004–2019, from 13,000 km^2 during 1992–2003. Similar trends, although less pronounced, were identified throughout the United Kingdom, France and Germany in both periods.

The Netherlands and Denmark, two key agricultural producers in Europe (Van Grinsven et al., 2012), showed an overall reduction in the predicted groundwater NO$_3^-$ concentrations since the implementation of the ND until 2003, followed by an increase in the subsequent years. These trends align with previous findings by for the Netherlands (Van Grinsven et al., 2016) (e.g., NO$_3^-$ concentrations are higher in the sandy soils) (Fig. 2) and for Denmark (Hansen et al., 2012). In Belgium, Flanders and Wallonia, there were moderate increasing and decreasing trends, respectively.

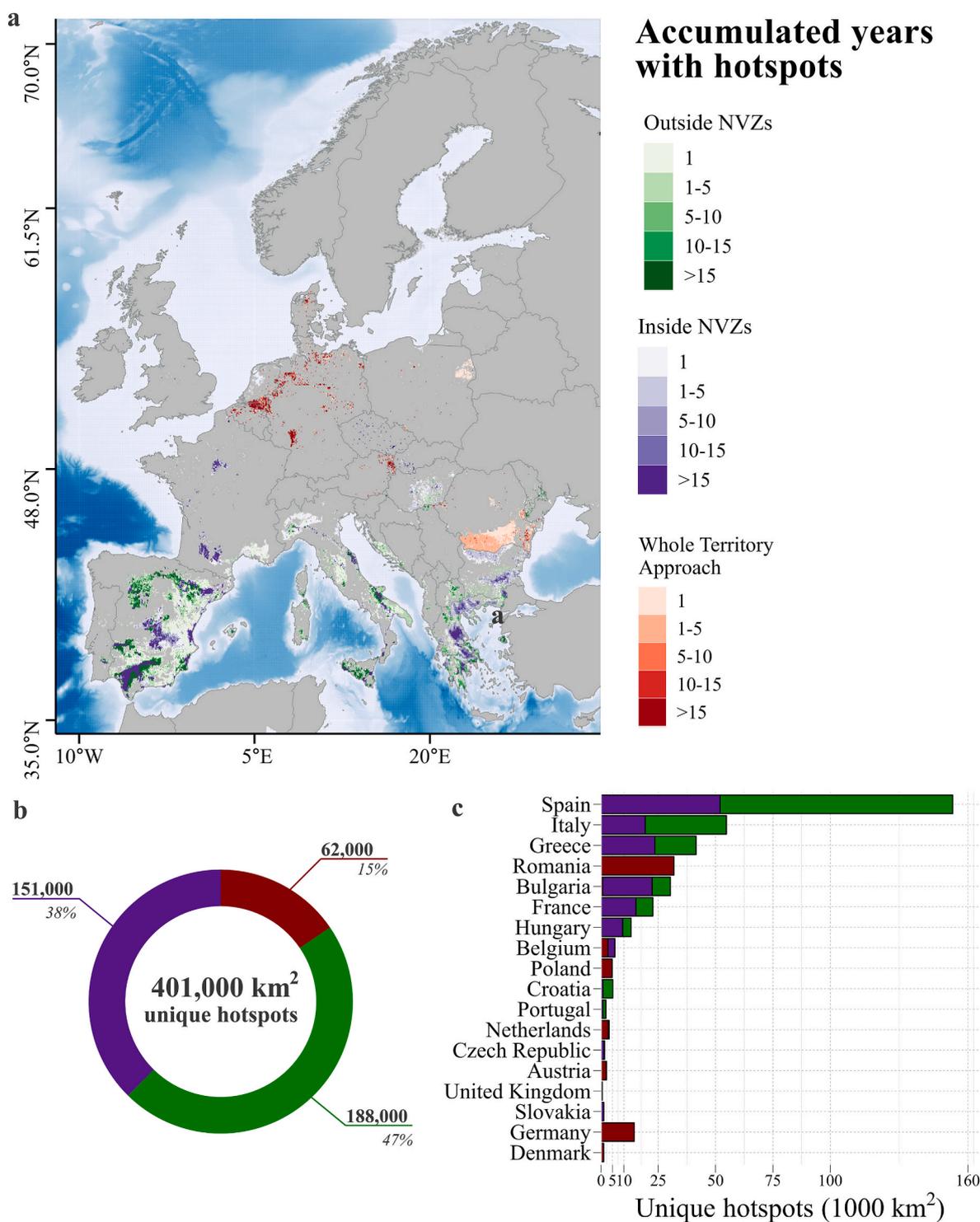**Fig. 5.** a) Spatial variation of total accumulated hotspots over Europe during the period 1992–2019. b) and c) showcase the total accumulated hotspots at the European and national levels, respectively. Three spatial units were used: inside the NVZs, outside the NVZs and whole territory approach. The numbers refer to the sum of years where a given cell attained concentrations >50 mg L^{-1}, thus representing unique hotspots.

The shift in the trends of the predicted groundwater NO_3^- concentration, from decreasing after the implementation of the ND until 2003, to an increase in the following years, appears to be in line with the trends simulated in the hotspots in Europe. Our findings thus raise the question of whether similar patterns can also be found inside and outside NVZs and whether the NVZs have been successfully covering hotspots in groundwater.

3.3. Are the Nitrate Vulnerable Zones being successful in targeting nitrate pollution in groundwater?

Our trend analysis for the NVZs for two distinct periods (1992–2003, 2004–2019) and the whole monitoring period of 1992–2019 is displayed in Fig. 4. Here we show a limited, and often contrasting, effectiveness across all NVZs in Europe. We found significant increasing trends in 21,000 of the 24,000 km^2 of hotspots that attained an increasing trend (>0.1 mg L^{-1} yr^{-1}). The largest statistically significant declining and increasing trends were also located in the regions inside rather than outside the NVZs. The area with increasing trends over 0.3 mg L^{-1} yr^{-1} increased almost five times, from 26,000 to 127,000 km^2, between 1992-2003 and 2004–2019. In parallel, areas with reductions higher than 0.3 mg L^{-1} yr^{-1} decreased by more than a factor of five (102,000 to 16,000 km^2). We also found an aggravation of the general trends outside the NVZs between these periods. Increasing trends expanded in almost 145,000 km^2 while decreasing trends contracted in almost the same

proportion (130,000 km^2). The trend reversal occurred in a number of NVZs across Europe, particularly in NW and Southern Europe.

The trends varied strongly per country, significantly decreasing over the whole period in Portugal, Denmark and the Netherlands and increasing in Greece, Croatia and Germany (Table S2). Our results are in agreement with the general magnitude and trends identified in NVZs in Portugal (Cameira et al., 2021; Serra et al., 2023a,b), Italy (Ducci et al., 2020; Frollini et al., 2021; Musacchio et al., 2020) and Spain (Arauzo and Martínez-Bastida, 2015; Orellana-Macías et al., 2020; Urresti-Estala et al., 2016). Nonetheless, assessing the NVZs only based on their trend is insufficient given the objective is to reduce the magnitude of hotspots to a level below the threshold of 50 mg L^{-1}. That is, decreasing trends are necessary but may be insufficient for NO_3^- concentrations in groundwater to decline to the point where water quality targets are met.

We analysed the distribution of hotspots across Europe (Fig. 5). We identified 401,000 km^2 of unique hotspots in Europe (cells that attained a NO_3^- concentration of more than 50 mg L^{-1} in at least one year). Our model revealed that 47% of the hotspots, or 188,000 km^2, were outside of the designated NVZs in Europe after the implementation of the ND, mainly in Spain (54%), Italy (21%) and Greece (11%). The most persistent hotspots (>15 years) were often in the vicinities of the designated NVZs around the Mediterranean Sea. We highlight Spain (e. g., Guadlquivir, Extremadura and Ebro basin), the Italian islands in the Mediterranean Sea (e.g., Sicily, Sardinia) and Central/Western Greece. Our results agree with the latest ND report for the period 2016–2019
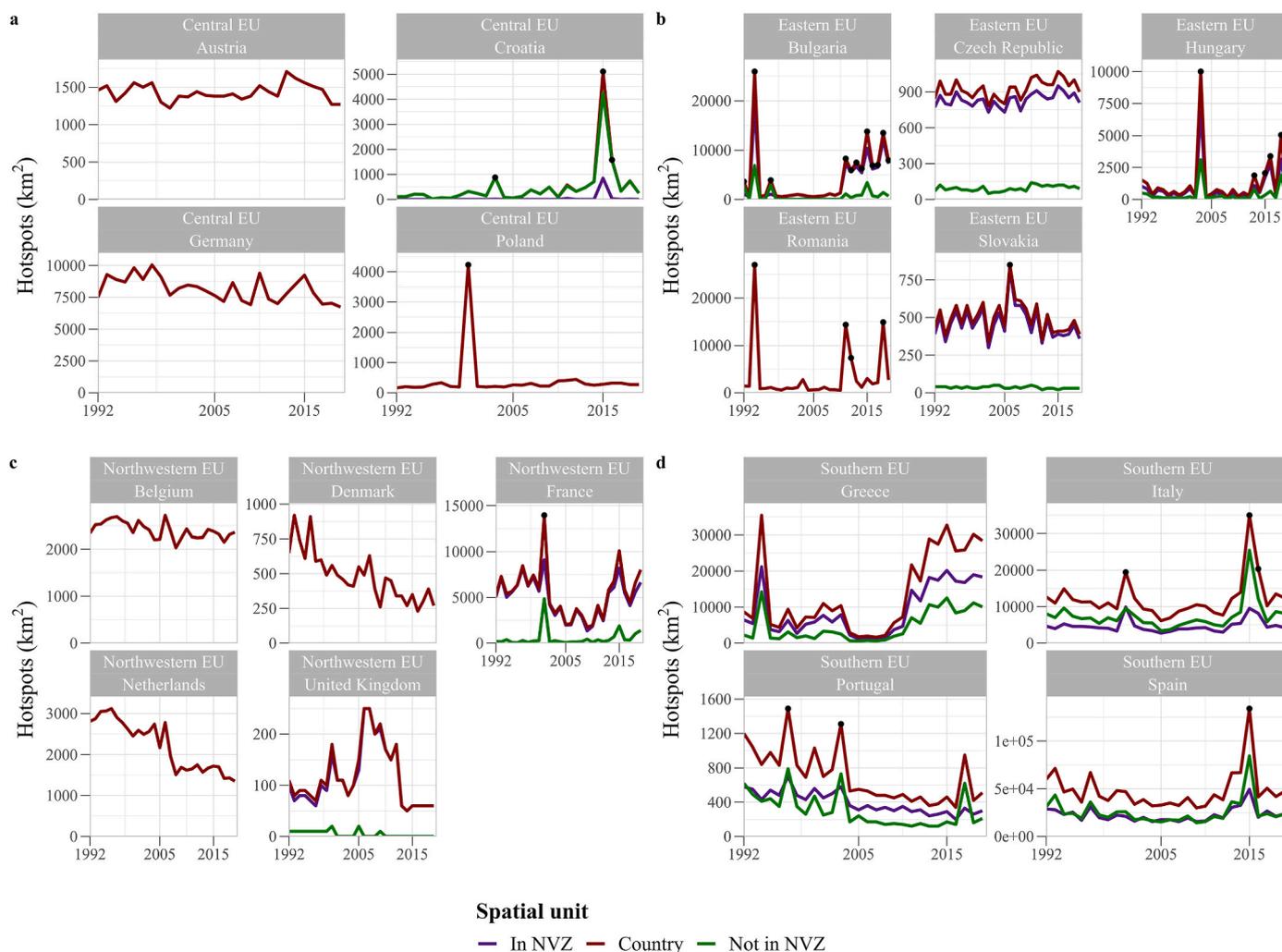

Fig. 6. Hotspot area inside and outside NVZs, and total per country during the period 1992–2019 in (a) Central Europe, (b) Eastern Europe, (c) Northwestern Europe and (d) Southern Europe. The black points represent years where outliers were detected.

(European Commission, 2021) that some NVZs appear to be insufficient to adequately cover the whole extent of NO_3^- hotspots, particularly in Hungary, Italy and Spain.

We computed the area of annual hotspots for each country (Fig. 6). Our results show that the Netherlands and Portugal were successful in reducing hotspot area by 50% during the period 1992–2019. This is indicated by a declining rate of 25 ($p = 0.001$) and 67 km^2 yr^{-1} ($p = 0.02$) for Portugal and the Netherlands, respectively. However, the NVZs in Portugal failed to capture 43% of the hotspots. Hotspot area also significantly declined in Denmark ($p = 0.001$) and Belgium ($p = 0.01$) by 17 and 12 km^2 yr^{-1}, respectively.

Spain was the European country with the largest hotspot area (48,000 $\pm$ 20,000 km^2 yr^{-1}). We estimated a decline in hotspots of 19 km^2 yr^{-1} for the entire period but with an increase after 2004 of 1262 km^2 yr^{-1} ($p = 0.001$). We predicted a hotspot area of 12,000 $\pm$ 6000 km^2 yr^{-1} for Italy, which did not exhibit any significant trend for 1992–2019. The NVZs in both Spain and Italy, which cover 24 and 15% of the country, respectively, contained only 47 and 39% of the hotspots, respectively (Fig. 7; Table S3). Our findings suggest that these countries could potentially improve their NVZ designations, as recommended by European Commission (2021). Conversely, France achieved a hotspot coverage of 92% despite no significant trend being detected for the entire period.

Germany obtained a declining trend of 7500 km^2 yr^{-1} during 1992–2019 ($p = 0.003$), suggesting a successful adoption of a whole-territory approach. We compared the average hotspot size in Germany with Knoll et al. (2020) for the period 2009–2018. Knoll et al. (2020) estimated a hotspot size of about 35,000 km^2, which is larger more than three times higher than our estimate (11,000 km^2). The main difference can be attributed to a hotspot cluster predicted in the Bavaria region (Southeastern Germany) by Knoll et al. (2020), while our predictions suggest that these clusters have concentrations in the range 25–40 mg L^{-1}. This may be explained by the improved spatial resolution from Knoll et al. (2020) of 1 km $\times$ 1 km, which enhances hotspot identification relative to our predictions of roughly 3 km $\times$ 3 km. Nonetheless, our model obtained a better performance for Germany (R^2 of 0.92, RMSE of 8 mg L^{-1}) than Knoll et al. (2020) (R^2 of 0.51, RMSE of 21 mg L^{-1}). Other countries in Central and Eastern Europe, such as Poland, Czech Republic, Bulgaria, and Greece, also showed statistically significant increasing trends. These countries generally achieved a higher hotspot coverage than countries in Western Europe (e.g., Portugal, Spain). We note, however, the growth in hotspot area simulated in Greece, which has increased from 2 to 19,000 km^2 between 2008 and 2019.

We also highlight some annual outliers that occurred at the grid level and have overestimated the hotspot areas at the European and national

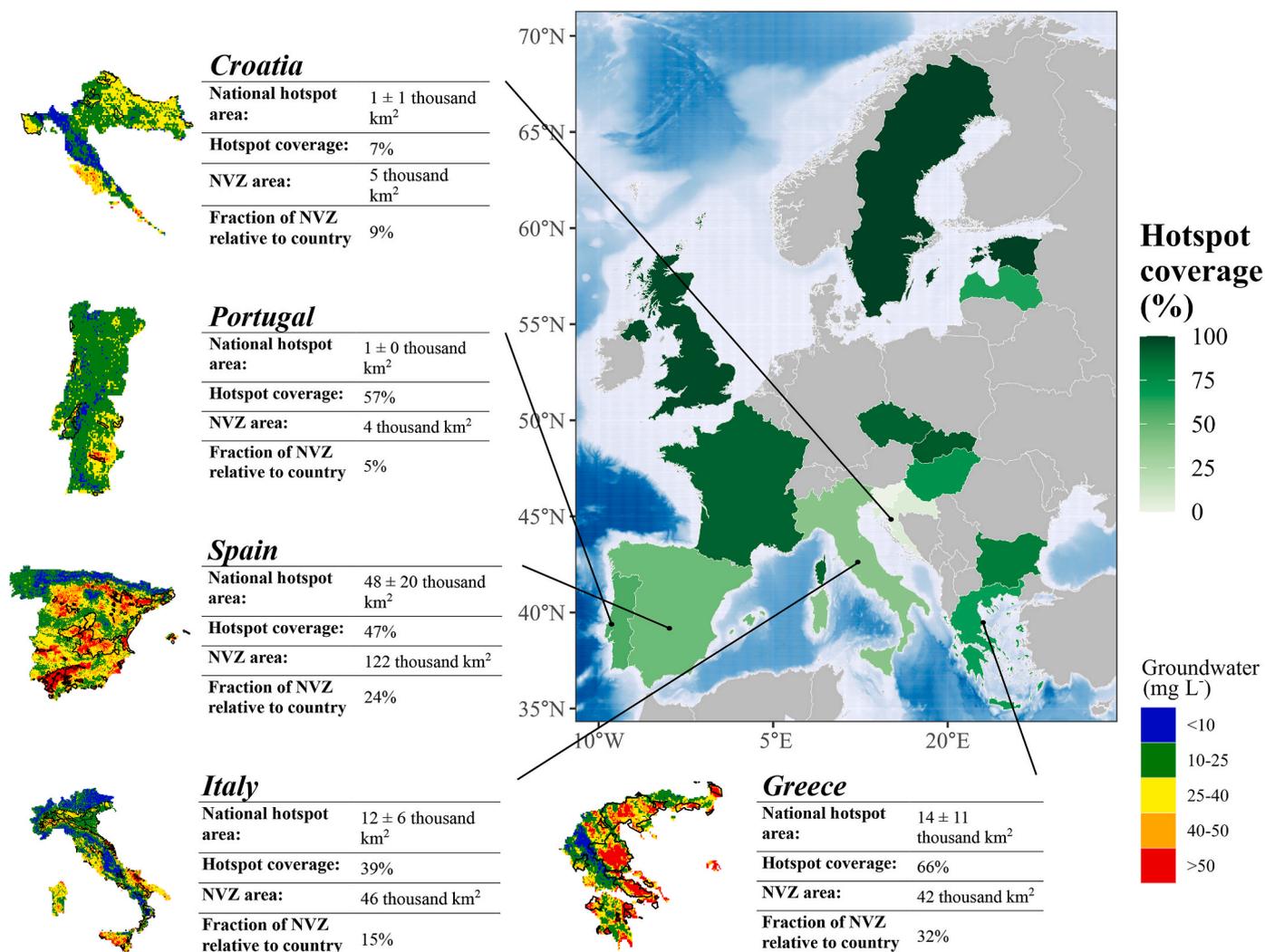**Fig. 7.** Hotspot coverage at the national level for MS without a Whole Territory Approach (WTA) implementation for the period 1992–2019. We provide a more detailed analysis for selected countries in Mediterranean Europe with relatively low hotspot coverage and/or large NO_3^- hotspots: Croatia, Portugal, Spain, Italy and Greece. For each country we also provide the averaged NO_3^- concentration in groundwater for 1992–2019.

levels. These occurred in different specific regions in different years (Fig. 6; Figs. S9–10), noted by a large increase in the average groundwater NO$_3^-$ concentration followed by a sharp decline in the following year (e.g., Croatia and Spain in 2015, Bulgaria in 1994). This was reflected in the national hotspot area, which sometimes increased more than five times (e.g., 750 km^2 in 2014–5000 km^2 in 2015 in Croatia). However, it is unclear whether the outliers are artefacts from a combination of the lack of predictive power of the random forest and/or uncertainty in data inputs and the biases induced by the marked differences in the availability of monitoring stations. It is also possible that some of these regions contain overlapped semi-confined and confined aquifers, for which the data does not specify, further biasing the predictions.

3.4. Exploring the heterogeneous effectiveness of the Nitrate Vulnerable Zones

Here we show that groundwater NO$_3^-$ concentrations are not declining uniformly across Europe, if at all. We explored the potential impact of the ND in N management by conducting scenario and uncertainty analyses targeting the N predictors. Our scenario simulations using N predictors from the historical (1961–1990) and present (2000–2019) conditions did not show any statistically significant differences ($p = 0.73$) relative to the baseline in Europe (Tables S4–5). We nonetheless found statistically significant differences at the national level (Tables S6–7 and Fig. S13). For instance, hotspot area would be 30% and 15% lower in France and Austria, respectively, if the N predictors stayed the same as during the historical scenario. Contrastingly, Portugal and the Netherlands demonstrated the impact of reducing N predictors over time as the hotspot area in the historical scenario were 65% and 45% lower than the baseline, respectively.

Our uncertainty analysis targeting the N predictors showed similar results, with an average uncertainty of −6%–8% in Europe (Fig. S14), but with an unequal spatial distribution as well as differences among N predictors (Fig. S15). The combined effect in uncertainty of N predictors ranged from negligible (−2%–2%) to substantial (−20%–40%). For instance, while the N surplus showed a large uncertainty in the Netherlands (average ranging between −15% and 32%), its importance was considerably lower in France (−1%–1%) or Portugal (−3%–3%). This shows the complexity of tackling N contamination through agricultural management and supports the conclusion of Klages et al. (2020) that there is no unified indicator for N management and water quality, requiring a careful examination of local factors.

The results from the scenario and uncertainty analyses point to a mixed effectiveness of the ND in reducing groundwater NO$_3^-$ hotspots at the European level. There is an untapped potential to further reduce hotspot area through N predictors in some countries, while others show a much slower response of hotspots to changes in N predictors. We are unable to specify the underlying cause for the trends or specifically benchmark the implications of the ND in most regions due to current data constraints such as of the development of the NVZs over time. Doing so would require detailed spatial information about designation and expansion dates for the different NVZs and the employment of hydrogeochemistry and isotopic characterizations across Europe (Biddau et al., 2019). However, the trends in hotspot area across Europe are likely to be a combination of factors such as the degree of enforcement and ambition of agro-environmental strategies, the impact of the agricultural transition into EU markets, time lags of NO$_3^-$ pollution responding to the implementation of regulations (Vero et al., 2018) and even the intensification-extensification dynamics in agriculture (Basu et al., 2022). The national implementation of the ND for EU15 only occurred in 1998, so the trends showed in Fig. 6 are unlikely to be an effect of the ND. Instead, the ND may have resulted in an increased awareness of farmers and other stakeholders about the value of N and the environmental and economic implications of N overapplication (Van Grinsven et al., 2016). This, together with higher N fertiliser prices may

have translated into the large decline of N fertilisers and N surplus across Europe (Van Grinsven et al., 2012) and in the general declining trend of the predicted NO$_3^-$ concentrations during 1992–2003 (Fig. 6).

The marked variation in NO$_3^-$ concentration trends in Europe is likely affected by the different timelines of environmental policies, regulations and awareness, institutional factors that constraint groundwater management, in combination with regional geohydrological characteristics. In some countries, such as Denmark, these reflect the spillover effects of earlier national policies implemented in the 1980s (Dalgaard et al., 2014). In other countries, particularly those in Eastern and Central Europe, the EU accession led to stricter environmental regulations, with a time-lag relative to older EU members. Conversely, we show the inability of the ND and other environmental policies to reduce NO$_3^-$ pollution in France (Fig. 7), among other countries, where long-term declining trends are still insufficient to meet water quality targets.

Groundwater vulnerability affects the effectiveness of policies and management practices in reducing NO$_3^-$ contamination (Hansen et al., 2017). The regions in Europe identified as having high groundwater vulnerability (Nistor, 2019) are consistent with those experiencing either increasing trends (e.g., France) or unable to significantly decrease NO$_3^-$ hotspots such as in Spain or Italy. The hydrologic time-lag of aquifers could explain why the NO$_3^-$ and N surplus hotspots (Batool et al., 2022) may not be synchronized across Europe, together with systematic errors in the predictors (e.g., geometric distortions, uncertainty in key statistical data used to constrain the N predictors and other biases implied from model assumptions), and differences in fertiliser type and gaseous losses.

Despite the overall decrease in N surpluses (Batool et al., 2022) and increase of the N use efficiency of many cropping systems (Lassaletta et al., 2014; Einarsson et al., 2021), we show these were insufficient to a widespread decrease of NO$_3^-$ contamination. Some regions are still experiencing the consequences of unrestrained N application in the 1960s–1980s as NO$_3^-$ accumulates in the vadose zone until reaching the water table (Ascott et al., 2017). This can take decades or even centuries in deep groundwater (Keuskamp et al., 2012). Long residence times also impacts the time-lag until improvements in agricultural practices are reflect in groundwater quality (Romero et al., 2016). Conversely, in regions with lower time-lags, reaching satisfatory reductions in groundwater quality can be achieved through N surpluses below historical levels to meet water quality goals established by the ND.

3.5. Path forward to meet nitrate water quality targets

Our findings point to an inadequate expansion of the designated NVZs in Europe, particularly after 2000. We illustrate how this expansion was insufficient to meet the NO$_3^-$ water quality objective of 50 mg L^{-1} in many regions. Although the ND does not establish any deadline for water quality objetives, good ecological and chemical status must be reached by 2027 per the Water Framework Directive. We show that only 16% of the 17,000 km^2 of hotspots in 2019 that attained a declining trend during 2004–2019 are likely to meet water quality standards in 2027 (Fig. 8a). We estimate that it would take 38 years until 50% of all hotspots of 2019 decrease until acceptable levels (<50 mg L^{-1}).

Reaching NO$_3^-$ quality targets in groundwater by 2027 is likely unattainable for most regions as it would require an average decrease of −2.4 ± 2.9 mg L^{-1} yr^{-1} in all hotspots of 2019 (Fig. 8b), rather distant from the current increasing rate of 2.6 ± 2.2 mg L^{-1} yr^{-1}. This means that 59% (71,000 km^2) and 15% (18,000 km^2) of current hotspots require an annual reduction larger than 1 and 5 mg L^{-1} to meet the target by 2027, respectively. For 2040, the average annual reduction required (−0.9 ± 1.1 mg L^{-1} yr^{-1}) would be closer to the current situation for hotspots with declining trend (−0.6 ± 0.8 mg L^{-1} yr^{-1}).

Here we aim to demonstrate the urgency to implement mitigation measures to minimize and maximize the expansion and reduction of hotspot areas, respectively. Even if mitigation measures are quickly implemented, we show the challenges imposed by the time-lag effect.
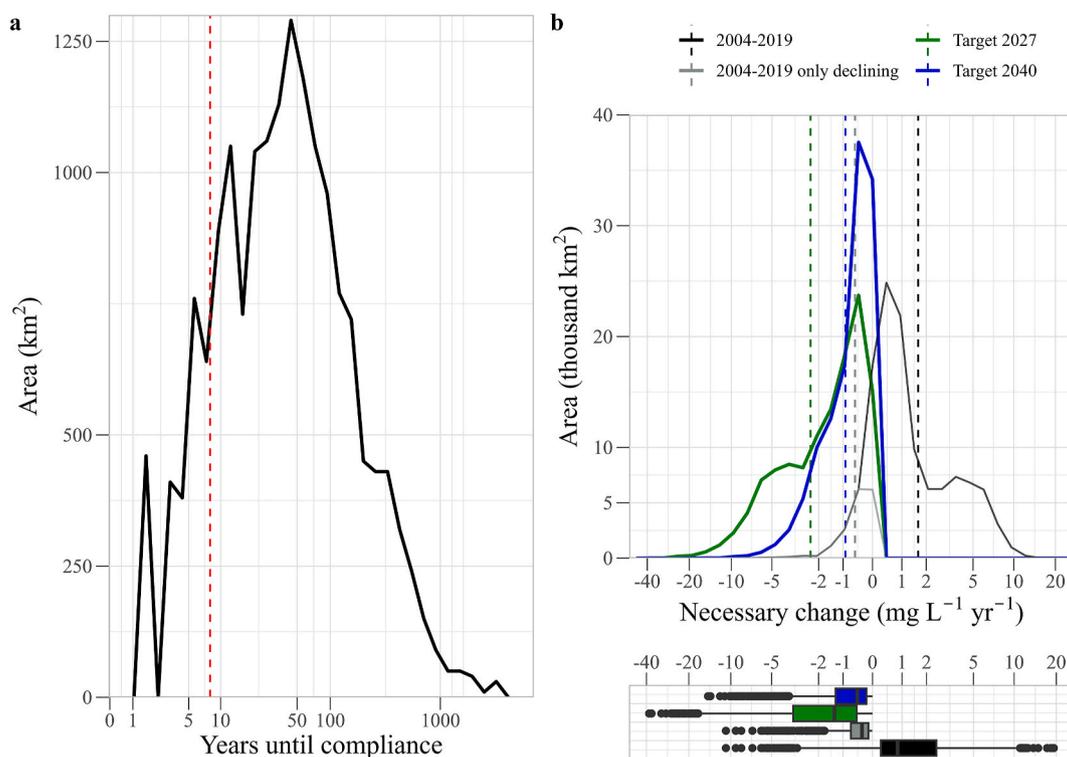
Fig. 8. a) Distribution of the time required until hotspots with declining trends in 2019 can comply with the water quality goal of 50 mg L^{-1}. The red dotted line represents the years until 2027. **b)** We explored the distribution of necessary changes that all hotspots in 2019 require to meet the water quality goal by 2027 and 2040. We also included the distribution of recent declining (grey) and all trends (black) for the period 2004–2019. Both a) and b) use a pseudo logarithmic scale in the x axis. (For interpretation of the references to colour in this figure legend, the reader is referred to the Web version of this article.)

However, suggesting policy and mitigation measures is outside the scope of this study. This requires a detailed examination of the main drivers of groundwater N contamination to implement site- and spatially explicit mitigation measures (Hashemi et al., 2018) as well as the collaboration between stakeholders, which can be challenging to achieve (Iversen et al., 2024).

3.6. Strengths and limitations of this approach

The predictive modelling approach here developed showed a good predictive performance (Fig. 1). Here we demonstrated the usefulness of large spatial scale modelling that allows the detection of NO$_3^-$ hotspots and respective trends across Europe at different spatial scales, while also providing a complete temporal series for each grid cell of groundwater NO$_3^-$ concentration. The output data here generated can be coupled with the predictors to detail the drivers behind groundwater NO$_3^-$ concentrations at the grid level. We acknowledge it is challenging to disentangle the drivers of NO$_3^-$ hotspots with the level of detail of local studies (e.g., Richard et al., 2018; Orellana-Macías et al., 2020) using this integrative large-scale approach. However, we argue its usefulness lies providing a harmonized overview at the continental scale in unifying hotspot detection and the designation of NVZs within the scope of the ND, overcoming the lack of standardization among MS. Our model also facilitates the assessment of the impact of different climatic and management exercises in terms of groundwater NO$_3^-$ concentration across Europe.

Although useful, this approach also has some limitations that still need to be overcome. We highlight the inherent uncertainty and quality of input data such as predictors and monitoring networks. Large spatial scale datasets seldom quantify and propagate uncertainty (e.g., Puy et al., 2023). We consider the data quality from monitoring networks collated from Waterbase to be a major limitation as sampling depths are often not distinguished and some regions were not adequately covered

by monitoring stations. Not being able to aggregate concentrations per depth can lead to inaccurate predictions, particularly in regions with overlaid aquifers (e.g., Brkić et al., 2021).

Data quality here refers to the spatial and temporal coverage across Europe and in a given monitoring site, respectively. Here we show the biases introduced by the annual variation in the annual stations available to train and evaluate the model. We demonstrate how the predictions are highly sensitive to the spatial coverage of national monitoring networks. In such regions (e.g., Croatia), the predictions may be unable to reflect the reality as per the national monitoring networks, especially if these differ markedly from the Waterbase data (Ondrasek et al., 2021). The extent to which the biases may have impacted the spatial predictions depends on several factors, of which we highlight the time-lag. Furthermore, it is also yet unclear of the underlying reasons for the outliers (i.e., overestimations) of groundwater NO$_3^-$ concentrations, but we speculate it is due to a combination of biases in the monitoring stations, uncertainty in data inputs and inability to properly include overlaid aquifers.

4. Conclusion

Here we explored the annual NO$_3^-$ concentration in groundwater across Europe for the period 1992–2019 using the random forests model. Our study reveals widespread hotspots in European groundwater, with statistically significant increasing trends in several regions. More importantly, our results indicate that only about half of the hotspots occur within the NVZs. This strongly suggests a need for additional efforts in monitoring and data analysis, and that NVZs may have to be substantially expanded in several MS. We highlight Southern Europe as a region with persistent hotspots over time, often in the vicinities of the currently designated NVZs.

While the implementation of the Nitrates Directive may have contributed to some reductions in hotspots, we demonstrate that

achieving significant reductions will often be impossible within a short time, due to the time-lags of NO_3^- contamination. Our predictive modelling approach Europe enables a site-specific multi-scaled examination of key regions that may need additional targeted strategies according to local conditions. This approach can enhance the monitoring and mitigation strategies of current MSbut also lead towards a more effective implementation of the Nitrates Directive of new MS by providing a cost-effective initial assessment of NVZ designation, priorities in the establishment of monitoring networks and the tailoring of good agricultural practices.

CRediT authorship contribution statement

J. Serra: Writing – review & editing, Writing – original draft, Visualization, Validation, Software, Methodology, Funding acquisition, Formal analysis, Data curation, Conceptualization. **C. Marques-dos-Santos:** Writing – review & editing, Supervision, Funding acquisition. **J. Marinheiro:** Writing – review & editing. **S. Cruz:** Writing – review & editing. **M.R. Cameira:** Writing – review & editing, Supervision, Funding acquisition. **W. de Vries:** Writing – review & editing, Formal analysis. **T. Dalgaard:** Writing – review & editing, Supervision. **N.J. Hutchings:** Writing – review & editing, Supervision. **M. Graversgaard:** Writing – review & editing, Formal analysis. **F. Giannini-Kurina:** Formal analysis, Methodology, Validation, Writing - review & editing. **L. Lassaletta:** Writing – review & editing, Validation, Formal analysis. **A. Sanz-Cobeña:** Writing – review & editing, Formal analysis. **M. Quemada:** Writing – review & editing, Formal analysis. **E. Aguilera:** Writing – review & editing, Validation, Formal analysis. **S. Medinets:** Writing – review & editing, Formal analysis. **R. Einarsson:** Writing – review & editing, Validation, Methodology, Formal analysis. **J. Garnier:** Writing – review & editing, Formal analysis.

Declaration of competing interest

The authors declare that they have no known competing financial interests or personal relationships that could have appeared to influence the work reported in this paper.

Data availability

Data is published in https://figshare.com/articles/dataset/_b_ Assessing_nitrate_groundwater_hotspots_in_Europe_reveals_a_severely_ inadequate_designation_of_Nitrate_Vulnerable_Zones_b_/24101001.

Appendix A. Supplementary data

Supplementary data to this article can be found online at https://doi.org/10.1016/j.chemosphere.2024.141830.

References

Arauzo, M., 2017. Vulnerability of groundwater resources to nitrate pollution: a simple and effective procedure for delimiting Nitrate Vulnerable Zones. Sci. Total Environ. 575, 799–812. https://doi.org/10.1016/j.scitotenv.2016.09.139.

Arauzo, M., Martínez-Bastida, J.J., 2015. Environmental factors affecting diffuse nitrate pollution in the major aquifers of central Spain: groundwater vulnerability vs. groundwater pollution. Environ. Earth Sci. 73, 8271–8286. https://doi.org/10.1007/s12665-014-3989-8.

Arauzo, M., Valladolid, M., Andries, D.M., 2022. Would delineation of nitrate vulnerable zones be improved by introducing a new parameter representing the risk associated with soil permeability in the Land Use–Intrinsic Vulnerability Procedure? Sci. Total Environ. 840 https://doi.org/10.1016/j.scitotenv.2022.156654.

Ascott, M.J., Gooddy, D.C., Wang, L., Stuart, M.E., Lewis, M.A., Ward, R.S., Binley, A.M., 2017. Global patterns of nitrate storage in the vadose zone. Nat. Commun. 8, 1–6. https://doi.org/10.1038/s41467-017-01321-w.

Basu, N.B., Van Meter, K.J., Byrnes, D.K., Van Cappellen, P., Brouwer, R., Jacobsen, B.H., Jarsjö, J., Rudolph, D.L., Cunha, M.C., Nelson, N., Bhattacharya, R., Destouni, G., Olsen, S.B., 2022. Managing nitrogen legacies to accelerate water quality improvement. Nat. Geosci. https://doi.org/10.1038/s41561-021-00889-9.

Batool, M., Sarrazin, F.J., Attinger, S., Basu, N.B., Van Meter, K., Kumar, R., 2022. Long-term annual soil nitrogen surplus across Europe (1850–2019). Sci. Data 9. https://doi.org/10.1038/s41597-022-01693-9.

Beusen, A.H.W., van Es, H.M., van Grinsven, H.J.M., Bouwman, L., McCrackin, M.L., Cassman, K.G., 2015. Losses of Ammonia and nitrate from agriculture and their effect on nitrogen recovery in the European union and the United States between 1900 and 2050. J. Environ. Qual. 44, 356. https://doi.org/10.2134/jeq2014.03.0102.

Biddau, R., Cidu, R., Da Pelo, S., Carletti, A., Ghiglieri, G., Pittalis, D., 2019. Source and fate of nitrate in contaminated groundwater systems: assessing spatial and temporal variations by hydrogeochemistry and multiple stable isotope tools. Sci. Total Environ. 647, 1121–1136. https://doi.org/10.1016/j.scitotenv.2018.08.007.

Brkić, Ž., Kuhta, M., Larva, O., Gottstein, S., 2019. Groundwater and connected ecosystems: an overview of groundwater body status assessment in Croatia. Environ. Sci. Eur. 31, 75. https://doi.org/10.1186/s12302-019-0261-6.

Brkić, Ž., Larva, O., Kuhta, M., 2021. Groundwater age as an indicator of nitrate concentration evolution I aquifers affected by agricultural activities. J. Hydrol. 602, 126799 https://doi.org/10.1016/j.jhydrol.2021.126799.

Cameira, M. do R., Rolim, J., Valente, F., Mesquita, M., Dragosits, U., Cordovil, C.M.d.S., 2021. Translating the agricultural N surplus hazard into groundwater pollution risk : implications for effectiveness of mitigation measures in nitrate vulnerable zones. Agric. Ecosyst. Environ. 306 https://doi.org/10.1016/j.agee.2020.107204.

Cameira, M.R., Rolim, J., Valente, F., Faro, A., Dragosits, U., Cordovil, C.M.d.S., 2019. Spatial distribution and uncertainties of nitrogen budgets for agriculture in the Tagus river basin in Portugal – implications for effectiveness of mitigation measures. Land Use Pol. 84, 278–293. https://doi.org/10.1016/j.landusepol.2019.02.028.

D'Haene, K., Salomez, J., De Neve, S., De Waele, J., Hofman, G., 2014. Environmental performance of nitrogen fertiliser limits imposed by the EU Nitrates Directive. Agric. Ecosyst. Environ. 192, 67–79. https://doi.org/10.1016/j.agee.2014.03.049.

Dalgaard, T., Hansen, B., Hasler, B., Hertel, O., Hutchings, N.J., Jacobsen, B.H., Jensen, L.S., Kronvang, B., Olesen, J.E., Schjørring, J.K., Kristensen, I.S., Graversgaard, M., Termansen, M., Vejre, H., 2014. Policies for agricultural nitrogen management-trends, challenges and prospects for improved efficiency in Denmark. Environ. Res. Lett. 9 https://doi.org/10.1088/1748-9326/9/11/115002.

DEFRA (Department for Environment, Food & Rural Affairs), 2016. Implementation of the nitrate pollution prevention regulations 2015 in England: method for designating nitrate vulnerable zones for groundwaters. Available at: https://assets.publishing.service.gov.uk/media/5a756b4040f0b6397f35e487/groundwater-nvz-methodology-2017-2020.pdf. (Accessed 28 November 2023).

Deng, Y., Ye, X., Du, X., 2023. Predictive modelling and analysis of key drivers of groundwater nitrate pollution based on machine learning. J. Hydrol. 624, 129934 https://doi.org/10.1016/j.jhydrol.2023.129934.

de Vries, W., Schulte-Uebbing, L., Kros, H., Voogd, J.C., Louwagie, G., 2021. Spatially explicit boundaries for agricultural nitrogen inputs in the European Union to meet air and water quality targets. Sci. Total Environ. 786, 147283 https://doi.org/10.1016/j.scitotenv.2021.147283.

Dorado-Guerra, D.Y., Corzo-Pérez, G., Paredes-Arquiola, J., Pérez-Martín, M.Á., 2022. Machine learning models to predict nitrate concentration in a river basin. Environ Res Commun 4. https://doi.org/10.1088/2515-7620/acabb7.

Ducci, D., Della Morte, R., Mottola, A., Onorati, G., Pugliano, G., 2020. Evaluating upward trends in groundwater nitrate concentrations: an example in an alluvial plain of the Campania region (Southern Italy). Environ. Earth Sci. 79 https://doi.org/10.1007/s12665-020-09062-8.

EEA (European Environmental Agency), 2021. WISE WFD Protected Areas under the Water Framework Directive. https://www.eea.europa.eu/en/datahub/datahubitem-view/06c3dcab-77bd-462b-b19e-32ac72d9155d. (Accessed 4 December 2023).

Einarsson, R., Sanz-Cobena, A., Aguilera, E., Billen, G., Garnier, J., van Grinsven, H.J.M., Lassaletta, L., 2021. Crop production and nitrogen use in European cropland and grassland 1961–2019. Sci. Data 8 (1), 288. https://doi.org/10.1038/s41597-021-01061-z.

European Commission, 2021. REPORT from the COMMISSION to the COUNCIL and the EUROPEAN PARLIAMENT on the Implementation of Council Directive 91/676/EEC Concerning the Protection of Waters against Pollution Caused by Nitrates from Agricultural Sources Based on Member State Reports for the Period 2016–2019.

European Commission, 2018. REPORT from the COMMISSION to the COUNCIL and the EUROPEAN PARLIAMENT on the Implementation of Council Directive 91/676/EEC Concerning the Protection of Waters against Pollution Caused by Nitrates from Agricultural Sources Based on Member State Reports for the Period 2012–2015.

Fannakh, A., Farsang, A., 2022. DRASTIC, GOD, and SI approaches for assessing groundwater vulnerability to pollution: a review. Environ. Sci. Eur. 34, 77. https://doi.org/10.1186/s12302-022-00646-8.

Frollini, E., Preziosi, E., Calace, N., Guerra, M., Guyennon, N., Marcaccio, M., Menichetti, S., Romano, E., Ghergo, S., 2021. Groundwater quality trend and trend reversal assessment in the European Water Framework Directive context: an example with nitrates in Italy. Environ. Sci. Pollut. Control Ser. 28, 22092–22104. https://doi.org/10.1007/s11356-020-11998-0/Published.

Garnier, J., Billen, G., Aguilera, E., Lassaletta, L., Einarsson, R., Serra, J., Cameira, M. do R., Marques-dos-Santos, C., Sanz-Cobeña, A., 2023. How much can changes in the agro-food system reduce agricultural nitrogen losses to the environment? Example of a temperate-Mediterranean gradient. J. Environ. Manag. 337 https://doi.org/10.1016/j.jenvman.2023.117732.

Haggerty, R., Sun, J., Yu, H., Li, Y., 2023. Application of machine learning in groundwater quality modelling – a comprehensive review. Water Res. 233, 119745 https://doi.org/10.1016/j.watres.2023.119745.

Hansen, A.L., Refsgaard, J.C., Olesen, J.E., Børgesen, C.D., 2017. Potential benefits of a spatially targeted regulation based on detailed N-reduction maps to decrease N-load from agriculture in a small groundwater dominated catchment. Sci. Total Environ. 595, 325–336. https://doi.org/10.1016/j.scitotenv.2017.03.114.

Hansen, B., Dalgaard, T., Thorling, L., Sørensen, B., Erlandsen, M., 2012. Regional analysis of groundwater nitrate concentrations and trends in Denmark in regard to agricultural influence. Biogeosciences 9, 3277–3286. https://doi.org/10.5194/bg-9-3277-2012.

Hashemi, F., Olesen, J.E., Jabloun, M., Hansen, A.L., 2018. Reducing uncertainty of estimated nitrogen load reductions to aquatic systems through spatially targeting agricultural mitigation measures using groundwater nitrogen reduction. J. Environ. Manag. 218, 451–464. https://doi.org/10.1016/j.jenvman.2018.04.078.

Huang, G., Liu, C., Sun, J., Zhang, M., Jing, J., Li, L., 2018. A regional scale investigation on factors controlling the groundwater chemistry of various aquifers in a rapidly urbanized area: a case study of the Pearl River Delta. Sci. Total Environ. 625, 510–518. https://doi.org/10.1016/j.scitotenv.2017.12.322.

Iversen, S.V., Dalgaard, T., Graversgaard, M., 2024. Discordance between farmers and scientists - perspectives on nitrogen reduction measures in Denmark. J. Environ. Manag. 352, 119877 https://doi.org/10.1016/j.jenvman.2023.119877.

Jain, H., 2023. Groundwater vulnerability and risk mitigation: a comprehensive review of the techniques and applications. Groundwater for Sustainable Development 22, 100968. https://doi.org/10.1016/j.gsd.2023.100968.

Jones, E.R., van Vliet, Qadir, M., Bierkens, M.F.P., 2021. Country-level and gridded estimates of wastewater production, collection, treatment and reuse. Earth Syst. Sci. Data 13 (2), 237–254. https://doi.org/10.5194/essd-13-237-2021.

Kazakis, N., Voudouris, K.S., 2015. Groundwater vulnerability and pollution risk assessment of porous aquifers to nitrate: modifying the DRASTIC method using quantitative parameters. J. Hydrol. (Amst.) 525, 13–25. https://doi.org/10.1016/j.jhydrol.2015.03.035.

Keuskamp, J.A., van Drecht, G., Bouwman, A.F., 2012. European-scale modelling of groundwater denitrification and associated N2O production. Environ. Pollut. 165, 67–76. https://doi.org/10.1111/j.1600-048X.2012.05551.x.

Karimanzira, D., Weis, J., Wunsch, A., Ritzau, L., Liesch, T., Ohmer, M., 2023. Application of machine learning and deep neural networks for spatial prediction of groundwater nitrate concentration to improve land use management practices. Frontiers in Water 5. https://doi.org/10.3389/frwa.2023.1193142.

Klages, S., Heidecke, C., Osterburg, B., Bailey, J., Calciu, I., Casey, C., Dalgaard, T., Frick, H., Glavan, M., D'Haene, K., Hofman, G., Leitão, I.A., Surdyk, N., Verloop, K., Velthof, G., 2020. Nitrogen surplus-a unified indicator for water pollution in Europe? Water (Switzerland) 12. https://doi.org/10.3390/W12041197.

Knoll, L., Breuer, L., Bach, M., 2019. Large scale prediction of groundwater nitrate concentrations from spatial data using machine learning. Sci. Total Environ. 668, 1317–1327. https://doi.org/10.1016/j.scitotenv.2019.03.045.

Knoll, K., Breuer, L., Bach, M., 2020. Nation-wide estimation of groundwater redox conditions and nitrate concentrations through machine learning. Environ. Res. Lett. 15, 064004 https://doi.org/10.1088/1748-9326/ab7d5c.

Lassaletta, L., Billen, G., Grizzetti, B., Anglade, J., Garnier, J., 2014. 50 year trends in nitrogen use efficiency of world cropping systems: the relationship between yield and nitrogen input to cropland. Environ. Res. Lett. 9 https://doi.org/10.1088/1748-9326/9/10/105011.

Musacchio, A., Re, V., Mas-Pla, J., Sacchi, E., 2020. EU Nitrates Directive, from theory to practice: environmental effectiveness and influence of regional governance on its performance. Ambio 49, 504–516. https://doi.org/10.1007/s13280-019-01197-8.

Nistor, M.M., 2019. Groundwater vulnerability in Europe under climate change. Quat. Int. https://doi.org/10.1016/j.quaint.2019.04.012.

Ondrasek, G., Begić, H.B., Romić, D., Brkić, Ž., Husnjak, S., Kovačić, M.B., 2021. A novel LUMNAqSoP approach for prioritising groundwater monitoring stations for implementation of the Nitrates Directive. Environ. Sci. Eur. 33, 23. https://doi.org/10.1186/s12302-021-00467-1.

Orellana-Macías, J.M., Merchán, D., Causapé, J., 2020. Evolution and assessment of a nitrate vulnerable zone over 20 years: gallocanta groundwater body (Spain). Hydrogeol. J. 28, 2207–2221. https://doi.org/10.1007/s10040-020-02184-0.

Ouedraogo, I., Defourny, P., Vanclooster, M., 2019. Application of random forest regression and comparison of its performance to multiple linear regression in modeling groundwater nitrate concentration at the African continent scale. Hydrogeol. J. 27, 1081–1098. https://doi.org/10.1007/s10040-018-1900-5.

Pearson, R.K., Neuvo, Y., Astola, J., Gabbouj, M., 2016. Generalized hampel filters. EURASIP J. Appl. Signal Process. 87 https://doi.org/10.1186/s13634-016-0383-6.

Puy, A., Sheikholeslami, R., Gupta, H.V., Hall, J.W., Lankford, B., Piano, S.L., Meier, J., Pappenberger, F., Porporato, A., Vico, G., Saltelli, A., 2023. The delusive accuracy of global irrigation water withdrawal estimates. Nat. Commun. 13, 3183. https://doi.org/10.1038/s41467-022-30731-8.

Quemada, M., Baranski, M., Nobel-de Lange, M.N.J., Vallejo, A., Cooper, J.M., 2013. Meta-analysis of strategies to control nitrate leaching in irrigated agricultural systems and their effects on crop yield. Agric. Ecosyst. Environ. 174, 1–10. https://doi.org/10.1016/j.agee.2013.04.018.

Ransom, K.M., Nolan, B.T., Stackelberg, P.E., Belitz, K., Fram, M.S., 2022. Machine learning predictions of nitrate in groundwater used for drinking supply in the conterminous United States. Sci. Total Environ. 807–3, 151065 https://doi.org/10.1016/j.scitotenv.2021.151065.

Romero, E., Le Gendre, R., Garnier, J., Billen, G., Fisson, C., Silvestre, M., Riou, P., 2016. Long-term water quality in the lower Seine: lessons learned over 4 decades of monitoring. Environ. Sci. Pol. 58, 141–154. https://doi.org/10.1016/j.envsci.2016.01.016.

Richard, A., Casagrande, M., Jeuffroy, M., David, C., 2018. An innovative method to assess suitability of Nitrate Directive measures for farm management. Land Use Pol. 72, 389–401. https://doi.org/10.1016/j.landusepol.2017.12.059.

Serio, F., Miglietta, P.P., Lamastra, L., Ficocelli, S., Intini, F., De Leo, F., De Donno, A., 2018. Groundwater nitrate contamination and agricultural land use: a grey water footprint perspective in Southern Apulia Region (Italy). Sci. Total Environ. 645, 1425–1431. https://doi.org/10.1016/j.scitotenv.2018.07.241.

Serra, J., Cameira, M.R., Cordovil, C.M. dS., Hutchings, N.J., 2021. Development of a groundwater contamination index based on the agricultural hazard and aquifer vulnerability: application to Portugal. Sci. Total Environ. 772, 145032 https://doi.org/10.1016/j.scitotenv.2021.145032.

Serra, J., Marques-dos-Santos, C., Marinheiro, J., Aguilera, E., Lassaletta, L., Sanz-Cobeña, A., Garnier, J., Billen, G., de Vries, W., Dalgaard, T., Hutchings, N., do Rosário Cameira, M., 2023a. Nitrogen inputs by irrigation is a missing link in the agricultural nitrogen cycle and related policies in Europe. Sci. Total Environ. 889, 164249 https://doi.org/10.1016/j.scitotenv.2023.164249.

Serra, J., Paredes, P., Cordovil, CmS., Cruz, S., Hutchings, N.J., Cameira, M.R., 2023b. Is irrigation water an overlooked source of nitrogen in agriculture? Agric. Water Manag. 278 https://doi.org/10.1016/j.agwat.2023.108147.

Spijker, J., Fraters, D., Vrijhoef, A., 2021. A machine learning based modelling framework to predict nitrate leaching from agricultural soils across The Netherlands. Environ Res Commun 3, 045002. https://doi.org/10.1088/2515-7620/abf15f.

Szalińska, E., Orlińska-Woźniak, P., Wilk, P., 2018. Nitrate vulnerable zones revision in Poland—assessment of environmental impact and land use conflicts. Sustainability 10 (9), 3297. https://doi.org/10.3390/su10093297.

Urresti-Estala, B., Gavilán, P.J., Pérez, I.V., Cantos, F.C., 2016. Assessment of hydrochemical trends in the highly anthropised Guadalhorce River basin (southern Spain) in terms of compliance with the European groundwater directive for 2015. Environ. Sci. Pollut. Control Ser. 23, 15990–16005. https://doi.org/10.1007/s11356-016-6662-9.

Van Grinsven, H.J.M., Ten Berge, H.F.M., Dalgaard, T., Fraters, B., Durand, P., Hart, A., Hofman, G., Jacobsen, B.H., Lalor, S.T.J., Lesschen, J.P., Osterburg, B., Richards, K. G., Techen, A.K., Vertès, F., Webb, J., Willems, W.J., 2012. Management, regulation and environmental impacts of nitrogen fertilization in northwestern Europe under

the Nitrates Directive; A benchmark study. Biogeosciences 9, 5143–5160. https://doi.org/10.5194/bg-9-5143-2012.

Van Grinsven, H.J.M., Tiktak, A., Rougoor, C.W., 2016. Evaluation of the Dutch implementation of the nitrates directive, the water framework directive and the national emission ceilings directive. NJAS - Wageningen J. Life Sci. 78, 69–84. https://doi.org/10.1016/j.njas.2016.03.010.

Vero, S.E., Basu, N.B., Van Meter, K., Richards, K.G., Mellander, P.E., Healy, M.G., Fenton, O., 2018. Revue: L'état environnemental et les implications du décalage temporel du nitrate en Europe et Amérique du Nord. Hydrogeol. J. 26, 7–22. https://doi.org/10.1007/s10040-017-1650-9.

Vigiak, O., Grizzetti, B., Zanni, M., Aloe, A., Dorati, C., Bouraoui, F., Pistocchi, A., 2020. Domestic waste emissions to European waters in the 2010s. Sci. Data 7, 33. https://doi.org/10.1038/s41597-020-0367-0.

Wick, K., Heumesser, C., Schmid, E., 2012. Groundwater nitrate contamination: factors and indicators. J. Environ. Manag. 111, 178–186. https://doi.org/10.1016/j.jenvman.2012.06.030.

Wuijts, S., Claessens, J., Farrow, L., Doody, D.G., Klages, S., Christophoridis, C., Cvejić, R., Glavan, M., Nesheim, I., Platjouw, F., Wright, I., Rowbottom, J., Graversgaard, M., van den Brink, C., Leitão, I., Ferreira, A., Boekhold, S., 2021. Protection of drinking water resources from agricultural pressures: effectiveness of EU regulations in the context of local realities. J. Environ. Manag. 287 https://doi.org/10.1016/j.jenvman.2021.112270.

Zhang, M., Huang, G., Liu, C., Zhang, Y., Chen, Z., Wang, J., 2020. Distributions and origins of nitrate, nitrite, and ammonium in various aquifers in an urbanized coastal area, south China. J. Hydrol. 582, 124528 https://doi.org/10.1016/j.jhydrol.2019.124528.